



# Nitridation of a Si(100) surface by 100-1000 eV N<sup>+</sup>2 ion beams

著者	高岡 毅
journal or publication title	The Journal of chemical physics
volume	101
number	9
page range	8238-8245
year	1994
URL	<a href="http://hdl.handle.net/10097/47626">http://hdl.handle.net/10097/47626</a>

doi: 10.1063/1.468194

# Nitridation of a Si(100) surface by 100–1000 eV $\text{N}_2^+$ ion beams

I. Kusunoki, T. Takaoka, Y. Igari, and K. Ohtsuka<sup>a)</sup>

Research Institute for Scientific Measurements, Tohoku University Katahira 2-1-1, Aoba-ku, Sendai 980, Japan

(Received 9 December 1993; accepted 29 July 1994)

The nitridation mechanism of silicon at room temperature under exposure to 100–1000 eV  $\text{N}_2^+$  ion beams has been studied *in situ* in an ultrahigh vacuum apparatus using x-ray photoelectron spectroscopy. The increase of the nitrogen content in a surface layer as a function of the ion dose was described by a simple formula which was derived by assuming random occupation of the reaction sites in the penetration zone of the nitrogen atoms. A change of the binding energy and the width of the  $\text{N}1s$  x-ray photoelectron spectrum during the reaction was observed and discussed with the component ratio  $\text{N}/\text{Si}_{\text{reacted}}$ . The  $\text{Si}2p$  x-ray photoelectron spectra were deconvoluted into five components of  $\text{Si}(0)$ ,  $\text{Si}(1)$ ,  $\text{Si}(2)$ ,  $\text{Si}(3)$ , and  $\text{Si}(4)$  by curve fitting, where  $\text{Si}(n)$  represents the components of Si bonded to  $n$  nitrogen atoms. Their populations were dependent on the ion dose and the ion energy. The nitride layers formed in the Si surface with low energy beams of 100–200 eV had near-stoichiometric composition of  $\text{Si}_3\text{N}_4$ . With beams of energy higher than 300 eV, however, they were nonstoichiometric compounds  $\text{SiN}_y$  ( $y < 1.3$ ) which were mixtures of those components. The influence of the beam energy was observed by the chemical shifts of the  $\text{N}1s$  and  $\text{Si}2p$  peaks at the saturation of the N content.

## I. INTRODUCTION

Although low energy reactive ion beams have a great potential to produce new materials on surfaces at room temperature, chemical reactions of a surface with ion beams have been studied less extensively than thermal gas/surface reactions. We feel that reaction processes during irradiation by ion beams on surfaces should be further investigated with a view to producing materials with special properties, because the mechanism for the reaction with beam particles with a high kinetic energy may be different from that of the thermal reaction with an ambient gas. With this in mind, the formation of silicon nitride films on Si(100) surfaces by reaction with low energy  $\text{N}_2^+$  ion beams has been studied in the present work.

In the past, there have been many investigations on thermal reactions of a Si surface with  $\text{NH}_3$ ,  $\text{NO}$ , and  $\text{N}$  by a variety of techniques.<sup>1–7</sup> The thermal nitridation of the Si surface produces a film of a stoichiometric compound  $\text{Si}_3\text{N}_4$ . On the other hand, the nitridation of a Si surface with a low energy  $\text{N}_2^+$  beam has also been reported by some investigators,<sup>8–11</sup> but the number of such studies is much less than that on the thermal reaction. Especially in the low energy range 100–1000 eV, the reaction process has not been investigated in detail, though Kang's group<sup>10–12</sup> has recently investigated the reaction with low energy (<600 eV)  $\text{N}^+$  and  $\text{N}_2^+$  ion beams by Auger electron spectroscopy (AES), ultraviolet photoelectron spectroscopy (UPS), and x-ray photoelectron spectroscopy (XPS).

In this work, the nitridation process of a Si(100) surface under exposure to 100–1000 eV  $\text{N}_2^+$  beams was studied *in situ* in an ultrahigh vacuum (UHV) apparatus using XPS. The increase of the N content in the surface layer was measured as a function of the ion dose at five ion beam energies.

The curves for the rates were analyzed by a formula derived from a reaction mechanism proposed. Chemical shifts of the  $\text{Si}2p$  and  $\text{N}1s$  core levels were observed during the progress of the reaction. The effects of the incident beam energy were clearly observed in the  $\text{Si}2p$  and  $\text{N}1s$  XPS spectra. The  $\text{Si}2p$  spectra were analyzed by curve fitting.

## II. EXPERIMENT

This experiment was carried out in an imaging XPS analytical instrument equipped with an ion beam gun (Shimadzu–Kratos XSAM-i). For the XPS measurements, a  $\text{MgK}\alpha$  x-ray source (1253.6 eV) was usually used. The electron analyzer was operated in the fixed analyzer transmission (FAT) mode at a constant pass energy of 20 eV. The base pressure of the experimental chamber was  $2 \times 10^{-10}$  Torr.

A substrate (about  $15 \times 15 \times 0.5$  mm<sup>3</sup>) was cut from a commercially available polished Si(100) wafer ( $p$  type, 10  $\Omega$ ). A native oxide layer on the surface was removed by etching with hydrofluoric acid and rinsing with purified water. After this procedure, it was mounted on to a sample holder, transferred into vacuum, and attached to an ultra-high vacuum (UHV) manipulator of the XPS apparatus. By using a differentially pumped ion beam gun (minibeam I), the surface contamination was removed by  $\text{Ar}^+$ -ion sputtering at 3 keV. The cleanliness of the surface was checked by XPS, and the clean region on the surface was identified from an imaging map for the pure  $\text{Si}2p$  or  $\text{O}1s$  XPS spectra.

A nitrogen ion beam generated by the same ion gun was focused onto the clean region of the surface at room temperature. The ion beam, which was generated by electron impact of  $\text{N}_2$  gas at 100 eV, consists mostly of  $\text{N}_2^+$  ions, but a few percent  $\text{N}^+$  atomic ions are usually included. The working pressure during the beam irradiation was about  $5 \times 10^{-8}$  Torr. The energy of the beam was varied from 100 to 1000 eV, and the ion beam current was monitored through the sample. A typical ion current at 200 eV was about 0.1  $\mu\text{A}$ . The area of

<sup>a)</sup>Present address: Fujitsu Co., Kawasaki.

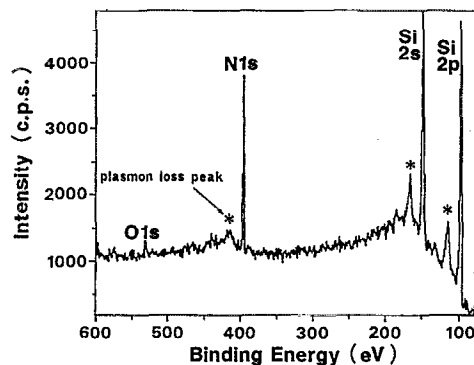


FIG. 1. A wide XPS spectrum of a nitrided Si surface.

nitride formation by the ion beam was measured from an elemental map of N obtained using the N1s XPS peak and was found to be about 3 mm<sup>2</sup> in size. The intensity distribution of the incident ions in the irradiation area could be estimated from the N1s XPS map taken with a 0.2 mm spatial resolution.

XPS spectra for the N1s and Si2p core levels were usually measured at the center of the beam spot with 0.6 mm spatial resolution. In estimating the N<sub>2</sub><sup>+</sup> dose, the intensity distribution over the irradiation area was also taken into account. Oxygen contamination on the surface was negligible until the middle stage of the reaction process. However, after beam exposures longer than several hours, a small oxygen peak was observed in an XPS spectrum taken in a wide energy range of 80–600 eV in binding energy.

The substrate was bombarded for a fixed time (>1 min) by the nitrogen ion beam at a given energy, and the XPS spectra of N1s and Si2p were measured with an energy resolution of about 1 eV at a normal electron emission angle. This procedure was repeated until the intensity of the N1s peak was saturated. To check the surface contamination, an XPS spectrum over the wide energy range was taken several times in a sequential procedure.

In order to check the bombardment effect of Ar<sup>+</sup> ions, we also used the Si(100) surfaces cleaned only by heating at 1000 °C in the UHV preparation chamber. These samples showed a 2×1 surface structure in a low energy electron diffraction (LEED) measurement as usual. The results obtained with these samples were very similar to the present ones. Then we concluded that the effect of the Ar<sup>+</sup>-ion sputtering does not bring any serious influence to the reaction mechanism described below.

### III. RESULTS

Upon exposure to the nitrogen ion beam, we can readily observe a peak due to N1s photoelectrons at a binding energy of 397 eV in the XPS spectra. Here, the binding energy is referred to a Fermi level, which was calibrated with the Ag(3d<sub>5/2</sub>) peak at 368.3 eV. Figure 1 shows a wide XPS spectrum obtained after the nitridation of the Si surface. The N1s, Si2s, and Si2p lines are comparably strong, the contaminant oxygen peak at 532 eV being very small. The N1s line is accompanied by a broad plasmon loss peak around

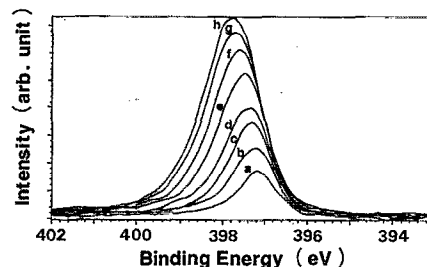


FIG. 2. Evolution of the N1s XPS spectrum during the nitridation of the Si(100) surface with the 200 eV ion beam. Amount of N<sub>2</sub><sup>+</sup> ion dose: (a) 0.25; (b) 0.5; (c) 1.0; (d) 1.5; (e) 2.0; (f) 2.5; (g) 3.5; and (h) 5.0×10<sup>15</sup> ions/cm<sup>2</sup>.

419 eV. The energy loss of 22 eV is correspondent to the creation of the bulk plasmon of the amorphous silicon nitride.<sup>13</sup>

Figure 2 shows some N1s XPS spectra at different stages of the nitridation of Si(100) with the 200 eV ion beams. The peak position of the N1s spectrum shifts from 397.1 eV toward higher binding energy with increasing N content, accompanied by broadening of the spectrum. The shapes of the spectra are a little asymmetric with a tailing toward higher binding energy.

In Fig. 3, the integrated intensities of the N1s spectra taken with the 100, 200, 300, 500, and 1000 eV ion beams are plotted as a function of the N<sub>2</sub><sup>+</sup> dose, which is the number of incident ions on 1 cm<sup>2</sup> of the surface. At all energies, the intensity of the N1s spectrum increases linearly with the dose in the initial stage, starts to saturate at a dose ~4×10<sup>15</sup> ions/cm<sup>2</sup>, and finally reaches a constant value. A similar dose dependence was also reported by Park *et al.*<sup>10</sup> In the present work, the intensities given in arbitrary units are normalized to the value at the saturation for the 200 eV ion beam. The relative values at the saturation for the different beam ener-

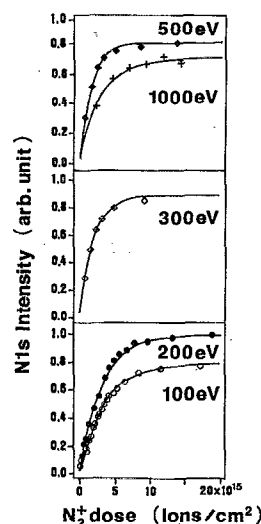


FIG. 3. N1s XPS intensity vs N<sub>2</sub><sup>+</sup> dose for various ion beam energies. The solid curves are obtained by Eq. (4). The parameters used are given in the text.

TABLE I. Relative intensities of the N1s XPS spectra obtained from the Si surfaces after saturation with N by bombarding with  $N_2^+$  ion beams at various energies.

Ion energy (eV)	100	200	300	500	1000
Relative intensity of the N1s peak	0.78	1.00	0.85	0.80	0.71

gies are given in Table I. There is a maximum at 200 eV, and thereafter the value decreases by  $\sim 30\%$  upon increasing the ion energy.

As seen in the spectra in Fig. 2, both the binding energy of the N1s core level and the full width at half-maximum (FWHM) of the spectrum increase with the  $N_2^+$  dose in the initial stage and reach constant values at the saturation of the nitrogen content. These constant values are dependent on the ion beam energy (see Fig. 7). The chemical shift of the line is the largest at 100 and 200 eV, and the binding energy reaches 397.8 eV. The FWHM of the peak at 100 eV changes from 1.0 to 1.8 eV. Upon increasing the ion energy, both the chemical shift and the linewidth at the saturation decrease. At 300, 500, and 1000 eV, the binding energies are 397.7, 397.55, and 397.35 eV, and the FWHMs are 1.5, 1.4, and 1.25 eV, respectively.

The Si2p XPS spectrum of the clean Si substrate shows a single peak at 99.4 eV with the FWHM of 1.2 eV. The spin-orbit splitting  $Si2p_{1/2}$  and  $Si2p_{3/2}$  is not resolved because the monochromatized x-ray source equipped was not used in the present experiments. Exposing the surface to the nitrogen ion beam, a tailing of the spectrum appears on the higher binding energy side. For the low energy beams of 100 and 200 eV, a separate peak builds up at the tail side with increasing N content in the surface layer. With increasing ion energy, however, the separation between the second peak and the elemental Si2p peak becomes less pronounced. At 1000 eV only, a broad peak tailing toward higher binding energy is observed. Figure 4 shows the Si2p XPS spectra measured at nitrogen saturation for the different beam energies. The binding energies at the second peaks formed for the 100 and 200 eV beams are in a range of 102.1–102.3 eV. The chemical shift of 2.7–2.9 eV from the elemental Si2p peak at 99.4 eV is a little larger than the 2.4–2.7 eV observed in amorphous- $Si_3N_4$  formed by chemical vapor deposition (CVD),<sup>14</sup> or electron cyclic resonance (ECR) plasma,<sup>15</sup> but lower than 3.8 eV for a  $Si_3N_4$  surface prepared by 20 keV  $N^+$  ion implantation.<sup>16</sup> Then we believe the binding energy at  $\sim 102.2$  eV is correspondent to that of the stoichiometric compound  $Si_3N_4$ . On the other hand, the tailing observed in the spectra for the higher beam energies suggests that the nitride layer consists of nonstoichiometric compounds of  $SiN_y$  ( $y < 1.3$ ).

The near stoichiometry ( $Si_3N_4$ ) for the films formed with the low energy (100–200 eV) beams is confirmed from the intensity ratio of the N1s peak to the chemically shifted Si2p peak, taking into account the relative sensitivities, as described below. Those facts suggest that the nitridation with the low energy beams proceeds completely to produce near-stoichiometric  $Si_3N_4$  film which has a sharp boundary with

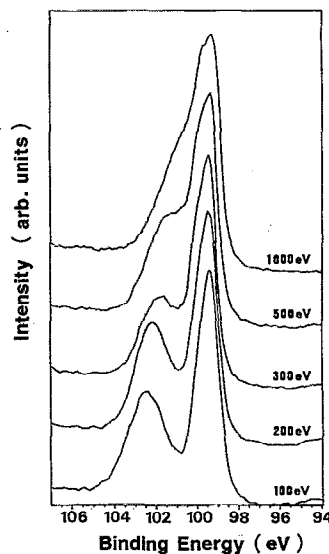


FIG. 4. Si2p XPS spectra obtained from nitrogen saturated surfaces for the different beam energies.

the Si substrate. The thickness of the film can be estimated using the intensity ratio of the chemically shifted Si2p peak to the elemental Si2p peak. When the mean free paths of the 1150 eV photoelectrons in Si and  $Si_3N_4$  are assumed to be 2.0 and 2.5 nm, respectively, from the empirical formula by Seah and Dench,<sup>17</sup> the thickness of the nitride layer at saturation is about 1.5 nm for the 200 eV beam. This is greater than 0.3–0.8 nm obtained for 500–3000 eV  $N_2^+$  beams by Jo *et al.*<sup>9</sup> or 0.6 nm for 100 eV by Park *et al.*<sup>10</sup> but in good agreement with 1.3 nm for 200 eV by Baek *et al.*<sup>11</sup> and comparable with 1.9 nm for 500 eV by Taylor *et al.*<sup>8</sup> From the thickness, the average reaction probability up to the dose of  $4 \times 10^{15}$  ions/cm<sup>2</sup> is estimated to be 0.7 using the nitrogen atomic concentration in  $Si_3N_4$  ( $\sim 5.9 \times 10^{22}$  N atoms/cm<sup>3</sup>), which is higher than that ( $\sim 0.25$ ) reported by others.<sup>8,10</sup> If we assume a different mean free path of 1.3 nm in Si,<sup>18</sup> the thickness becomes 1 nm. In this case, the reaction probability is 0.45.

The Si2p spectra taken during the reaction were analyzed by curve fitting. The spectra were tentatively decomposed into five components by procedures similar to those of Kärcher *et al.*<sup>13</sup> In the present work, the Si2p peak from a clean surface before the  $N_2^+$  beam irradiation is at the binding energy of 99.4 eV and its shape is approximately fitted by a Gaussian with a width of 1.19 eV (FWHM). Then we fix the line shape of the elemental Si2p peak from unreacted parts including the substrate. Four other components are correspondent to the Si– $Si_{4-n}N_n$  ( $n=1,2,3,4$ ) bonding configurations. Hereafter, they are denoted by Si( $n$ ). In the present analysis, for simplicity, the energy separation of each component is assumed to be equal as a consequence of the additivity of chemical shifts. Since the energy of the stoichiometric compound  $Si_3N_4$ , in which the Si atom is coordinated with four nitrogen atoms, is found at  $\sim 102.2$  eV, the binding energy of the Si( $n$ ) component is shifted toward higher energy by  $n \times 0.7$  eV from 99.4 eV. In a curve fitting named by

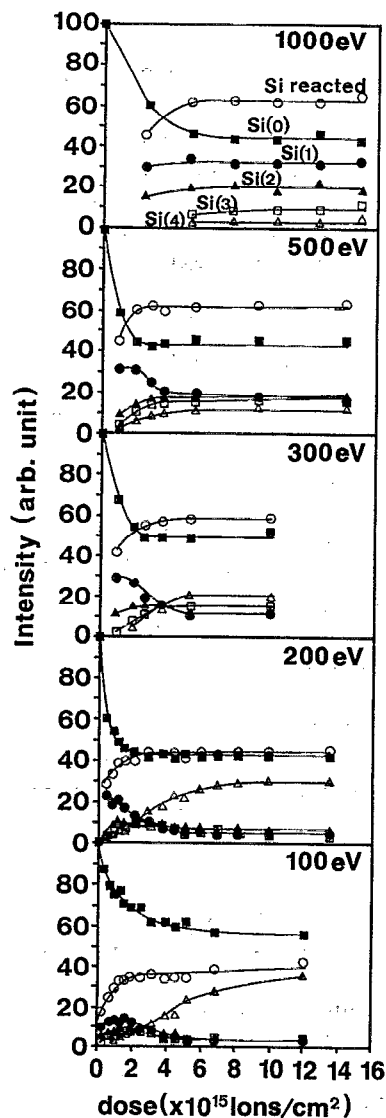


FIG. 5. Relative intensities of the five components [Si(0), Si(1), Si(2), Si(3), and Si(4)] and the summation [ $\Sigma$ Si( $n$ ),  $n=1-4$ ] as a function of the  $N_2^+$  dose. Solid squares indicate the data for Si(0), solid circles indicate data for Si(1), solid triangles indicate data for Si(2), open squares indicate data for Si(3), open triangles indicate data for Si(4), and open circles indicate data for the summation from Si(1) to Si(4).

type A, the line shape for every component is assumed to be the same as that of the elemental Si. In type B, the linewidth for the chemically shifted components ( $n \geq 1$ ) is assumed to be 1.9 eV (FWHM), the value of which is experimentally obtained by the present apparatus for a  $Si_3N_4$  fine powder supplied by the Nilaco Co. It is the same as that used in fit B by Kärcher *et al.*<sup>13</sup>

Curve fitting performed under these assumptions generally gives a similar spectrum to the experimental one, though some ambiguity and fitting errors remain in many cases. The results obtained by type B seem to be more reasonable in the present work than by type A. Then we present here the results by type B. The relative intensities of the components are plotted as a function of the  $N_2^+$  dose at the five beam energies in Fig. 5. The intensity of the Si(0) component de-

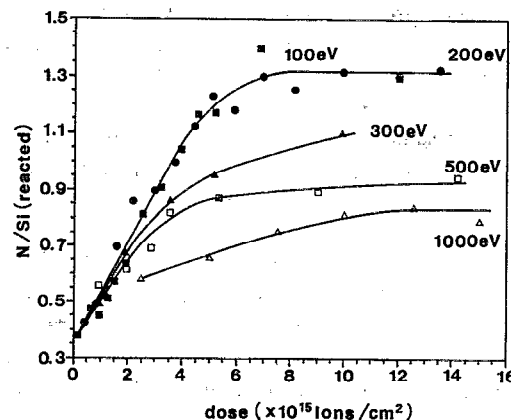


FIG. 6.  $N/Si_{\text{reacted}}$  as a function of the  $N_2^+$  dose. Solid squares indicate the data for 100 eV, solid circles indicate data for 200 eV, solid triangles indicate data for 300 eV, open squares indicate data for 500 eV, and open triangles indicate data for 1000 eV. The solid curves are guides to the eye.

creases rapidly in the initial stage and reaches a constant value at the saturation of the nitrogen content. The constant value comes from the photoelectrons emitted from the substrate under the reaction zone. The intensity of the nitride part separated from the elemental Si is hereafter denoted as  $I_{Si(\text{reacted})}$ , which is given by subtracting the Si(0) part from the whole spectrum or by adding the reacted components [ $\Sigma$  Si( $n$ ),  $n=1-4$ ]. The intensity curve of  $I_{Si(\text{reacted})}$  is in contrast with that of Si(0). It saturates at an ion dose between  $1-5 \times 10^{15}$  ions/cm<sup>2</sup>, which depends on the beam energy. The saturation value of  $I_{Si(\text{reacted})}$  increases with the ion energy, which indicates that the depth of the reaction zone increases with it. The Si(1) component appears in the initial stage and decreases upon increasing the ion dose, except for the 1000 eV case, and it takes a steady value at the saturation. At the low beam energies, the Si(2) and Si(3) components increase upon decreasing the Si(1) component in the early stage, and decrease upon increasing the Si(4) component. For the 100 and 200 eV beams, the Si(4) component finally becomes dominant in the reaction zone, which is expected from the spectra in Fig. 4. However, the curve fitting of type A for the same spectra gives a comparable ratio to the Si(3) and Si(4) components. This is unfavorable for the atomic ratio  $N/Si_{\text{reacted}}$  of about 1.3 at the saturation as described below, than the results by type B adopted here. In the curve fitting for 300 and 500 eV, the four components highly mix even in the final product. At 1000 eV, the intensity of the component ratio is in a sequence of Si(1) > Si(2) > Si(3) > Si(4) in the whole reaction process. The variation of the component ratios during the reaction is reflected to the peak shifts of the chemically shifted Si2p spectra.

The ratio of the nitrogen atoms to the reacted Si atoms is estimated by

$$x = (I_N/0.42)/(I_{Si(\text{reacted})}/0.27), \quad (1)$$

where 0.42 and 0.27 are the relative sensitivities of the N1s and the Si2p spectra, respectively.<sup>19</sup> Hereafter we denote the value  $x$  as  $N/Si_{\text{reacted}}$ . It should be noted that  $N/Si_{\text{reacted}}$  dif-

fers from the composition ratio  $N/Si(=y)$  in the film because unreacted Si atoms remain in the film especially in the beginning stage. Nevertheless,  $N/Si_{\text{reacted}}$  will be equal to the composition ratio  $N/Si$  at the nitrogen saturation. In a perfect crystal,  $x$  represents an average number of N atoms bonded to a Si atom. Then it should be 0.33 in a  $Si(Si_3N)$  form at the beginning of the reaction and 1.33 in the stoichiometric  $Si_3N_4$  form at nitrogen saturation. The values obtained for the different beam energies are plotted as a function of the ion dose in Fig. 6. At low energies, the ratio  $x$  increases with the ion dose and levels off with the nitrogen saturation at the ion dose about  $6 \times 10^{15}$  ions/cm<sup>2</sup>. The saturation values attained for the 100 and 200 eV beams are about  $x=1.3$ , which is in good agreement with  $x=1.33$  for  $Si_3N_4$ . The initial increase of the curve indicates that the average number of N atoms bonded to a Si atom increases with the N content. This is naturally acceptable, though Park *et al.*<sup>10</sup> found  $x$  values independent of the  $N_2^+$  dose. For the 300, 500, and 1000 eV beams, however, the  $x$  values at the saturation are limited to the lower value than 1.3, which suggests that the nitride layer is nonstoichiometric compounds. This is consistent with the analysis by curve fitting of type B.

#### IV. DISCUSSION

When a positive molecular ion with a single charge collides with a metal or semiconductor surface, it usually accepts an electron from the solid in the neighborhood of the surface and becomes neutralized with a high probability. The neutralized molecule, the kinetic energy of which will still be as high as that of the incident beam, collides violently with a surface atom and dissociates into some fragments on the surface with a certain probability. Since the dissociation energy of the  $N_2$  molecule is 9.76 eV, the fragment atoms produced even at 100 eV of the beam energy still have enough energy to penetrate into the solid. Some of the fragment atoms which satisfy a certain condition of impact parameter of collision with a surface atom can pass through the outermost layer of the surface. After a collision cascade in the solid, the atoms lose their kinetic energy and react with the nearest Si atoms. With the collision, the Si atoms are also displaced from their regular positions in the crystal. Thus a mixing layer of the N and Si atoms is formed in the surface. Those N atoms which do not encounter a reaction site will gradually migrate in the solid and may reach the surface again. Here isolated N atoms will recombine with each other and escape from the surface as  $N_2$  molecules into the gas phase. This escape process of unreacted N atoms occurs concurrently with the reaction and becomes dominant at the late stage of the nitridation process.

Let us consider the increasing rate of the  $N1s$  peak intensity shown in Fig. 3. As the maximum penetration depth of the N atom is limited by the incident beam energy, the volume of the reaction zone is fixed at a given energy. We define  $N_0$  as the number of reaction sites for N atoms in the reaction zone under a unit surface area.  $N$  is the number of the reacted N atoms in the volume at time  $t$  after starting the irradiation.  $F$  is the  $N_2^+$  beam flux multiplied by 2. Assuming that the reaction takes place randomly in the volume, we can express the rate equation for  $N$ ,

$$dN/dt = \sigma F(N_0 - N), \quad (2)$$

where  $\sigma$  is the apparent cross section for the reaction.

At higher energies, we must also consider the self-sputtering of N atoms on the surface during the beam irradiation. This phenomenon hinders the growth of the nitride film. If the number of N atoms existing on the surface is described by  $N/k$ , where  $k$  is the number of atomic layers in the reaction zone, Eq. (2) is modified as follows:

$$\begin{aligned} dN/dt &= \sigma F(N_0 - N) - sFN/k, \\ &= F[\sigma N_0 - (\sigma + s')N], \end{aligned} \quad (3)$$

where  $s$  is the apparent cross section of the sputtering,  $s/k$  being replaced by  $s'$ . The solution of Eq. (3) is given by

$$N(t) = [\sigma N_0 / (\sigma + s')] \{1 - \exp[-(\sigma + s')Ft]\}. \quad (4)$$

Here  $Ft$  is the total number of the incident nitrogen atoms per unit area until time  $t$ , which is twice the  $N_2^+$  ion dose. The experimental points of  $N$  as a function of the ion dose follow very well the curves calculated from Eq. (4) for all cases measured. The parameters of  $(\sigma + s')$  used for fitting are 1.2, 1.6, 2.3, 2.9, and  $1.6 \times 10^{-16}$  cm<sup>2</sup> at 100, 200, 300, 500, and 1000 eV, respectively. These values are comparable in order with the collisional cross sections in the gas phase.

From Eq. (4), the number of N atoms in the steady state at  $t = \infty$  is expressed by

$$N(\infty) = \sigma N_0 / (\sigma + s'). \quad (5)$$

Here both  $N_0$  and  $s'$  are expected to increase with ion energy in our energy regime, while  $s'$  can be neglected at low energy. The increase of  $s'$  may be greater than that of  $N_0$  in the high energy regime. Therefore, the value of  $N(\infty)$  in Eq. (5) has a maximum in the energy dependence. Experimentally the maximum is obtained at 200 eV as seen in Table I. Above this energy, the relative intensity of the  $N1s$  peak decreases with increasing incident beam energy.

This model of the reaction mechanism can be compared with that for the thermal reaction of Si with  $C_2H_2$ , which has been studied by us.<sup>20-22</sup> The reactant gas with thermal energy reacts with Si atoms in the top layer of the surface where the Si atoms are supplied by thermal diffusion from inside of the solid, while the reactive ions with kinetic energy of a few hundred electron volts penetrate into the solid and react with the Si atoms also in deeper layers. The reaction sites in the penetration zone may be randomly occupied by the N atoms in the initial stage and gradually ordered in short range.

Though we did not determine the crystal structure, the nitride film is probably amorphous. In the films produced at the lower ion energies, however, the local structure at the nitrogen saturation may be similar to  $\beta$ - $Si_3N_4$ ,<sup>23</sup> because the amorphous and crystalline nitrides have essentially the same short-range order. The electrical structure of the nitride is also expected to be similar to that of the microcrystal.<sup>24</sup>

Now let us consider the change of the electronic and bonding properties of the nitride layers during the reaction. As seen in Fig. 2, the  $N1s$  binding energy at the peak shifts toward higher energy upon increasing the nitrogen content in the layer. Such a shift has been observed by others.<sup>13,14,25</sup> Kärcher *et al.*<sup>13</sup> have suggested that it arises from a shift of

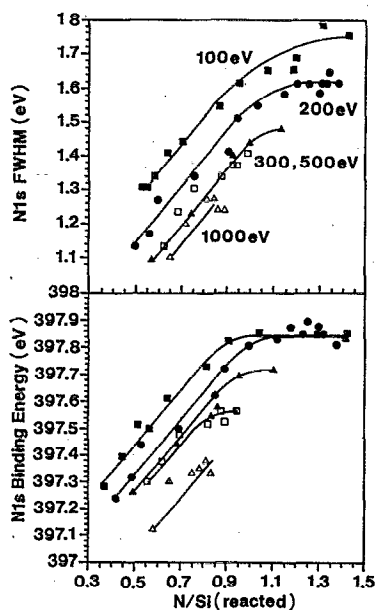


FIG. 7. The N1s binding energies and the FWHMs of the spectra as a function of the ratio  $N/Si_{\text{reacted}}$ . Solid squares indicate the data for 100 eV, solid circles indicate data for 200 eV, solid triangles indicate data for 300 eV, open squares indicate data for 500 eV, and open triangles indicate data for 1000 eV. The solid curves are guides to the eye.

the Fermi level, but in this experiment, the peak position of the elementary Si2p component from the underlying substrate was in the range of  $\pm 0.1$  eV from 99.4 eV. This is consistent with the recent result by Baek *et al.*<sup>11</sup> Therefore, the change of 0.8 eV observed for the N1s peak cannot be explained by the Fermi level shift alone.

In silicon nitride, the valence electrons 3p and 3s of the Si atoms are transferred onto the N atoms because the N atom is more electronegative than the Si atom. By a shield effect of the transferred valence electrons, the binding energy of the N1s state becomes lower than 402 eV of an isolated N atom. According to a theoretical prediction,<sup>26</sup> the binding energy of 397.0 eV corresponds roughly to the negatively charged state of  $N^{-\delta}$  ( $2.0 > \delta > 1.0$ ). If the total valence electrons of Si ( $2 \times 3p + 2 \times 3s$ ) were transferred onto the N2p orbitals as in an ionic crystal, the charge neutrality in  $Si_3N_4$  would be maintained in the form  $(Si^{+4})_3(N^{-3})_4$ . Since the bonding in the solid of  $Si_3N_4$  is of course covalent, the electron charges are shared among these atoms.

During the reaction, the ratio  $N/Si_{\text{reacted}}$  increases as seen in Fig. 6. In the initial stage, the N atoms will combine with the surrounding Si atoms which are not bonded to another N atom. Here the basic bond  $Si(Si_3N)$  is denoted by Si(1) as described before. In this configuration, the N atom can most effectively attract the valence electrons of the surrounding Si atoms. Increasing the N content, the number of nitrogen atoms bonded to a Si atom will change in sequence as  $Si(1) \rightarrow Si(2) \rightarrow Si(3) \rightarrow Si(4)$ . These changes induce a redistribution of the valence electrons between the Si and N atoms. With increasing  $n$ , the partial charge of the N atoms is reduced by sharing the valence electrons from the Si atoms

with other surrounding N atoms. As a result, the N1s binding energy rises. This is a so-called induction effect. As the position of the elemental Si2p peak from the substrate remains at  $\sim 99.4$  eV during the reaction, the peak shift observed in the N1s spectra (see Fig. 2) should be mainly attributed to this induction effect.

In Fig. 7, the binding energies of the N1s levels are plotted as a function of the ratio  $N/Si_{\text{reacted}}$ . The binding energy increases upon increasing the ratio and levels off for 100 and 200 eV. The increase rate is almost the same for every case, though the binding energies at the same value of  $N/Si_{\text{reacted}}$  are different. This is similar to a result given by Hasegawa *et al.*<sup>25</sup> According to their effective-charge analysis, the partial charge on a N atom per bonding unit changes from  $-0.30$  at  $x=0.33$  to  $-0.18$  at  $x=1.33$ . In an ideal case that the nitrogen is threefold silicon coordinated, the partial charge on a N atom will vary from  $-0.9$  to  $-0.54$ . Thus the binding energy of N1s increases with the nitrogen content. Upon increasing the ion beam energy, however, the N1s binding energy at the same value of  $N/Si_{\text{reacted}}$  decreases. These facts suggest that the nitride layers formed by different ion energies have different structures at the same ratio of  $N/Si_{\text{reacted}}$ . The high energy ions or atoms break the Si-Si bonding in the solid and create many defects along the path, and finally each of the N atoms bonds to three Si atoms in the neighborhood. In the nitride layer formed by the higher energy beams, most of the Si atoms bond to only one or two nitrogen atoms in spite of the high nitrogen contents as seen in Fig. 5. The defects around the Si atoms will reduce the induction effect for the N1s binding energy. This is a plausible reason for the low reduction of the chemical shift of the N1s level. Thus, the deviation from the ideal curve (i.e., the case for the lowest beam energy) may give a measure of the imperfection (interstitial N atoms, defects of Si atoms, and unsaturated bondings of Si) of the silicon nitride film.

The FWHMs of the N1s XPS spectra are also plotted as a function of the ratio  $N/Si_{\text{reacted}}$  in Fig. 7. The width increases with the N1s binding energy. The origin of the broadening of the spectrum is not clear, but it also reflects the chemical state of the product. In our measurements, the FWHM of the N1s spectrum for the fine powder of  $Si_3N_4$  embedded in a gold plate was 1.67 eV, which is in good agreement with the values observed for the 100 and 200 eV beams at the saturation.

Though we do not show the chemically shifted  $Si_{\text{reacted}}$  2p spectra which are obtained by subtracting the elemental Si(0) component from the observed Si2p spectrum, the intensity of the  $Si_{\text{reacted}}$  spectrum increases monotonically in the initial stage and saturates at an ion dose between  $1-4 \times 10^{15}$  ions/cm<sup>2</sup> as seen in the curves of  $Si_{\text{reacted}}$  in Fig. 5. The binding energy at the peak position of the  $Si_{\text{reacted}}$  spectrum shifts towards higher energy during the reaction by transferring the Si valence electrons onto the N atoms, and it reaches a constant energy at the saturation which depends on the ion energy. The final values for the nitride layers formed with the 100 and 200 eV beams are 102.1–102.4 eV for the binding energy and the FWHM of 2.0 eV, as expected for the near stoichiometric compound  $Si_3N_4$ . For the beams of energy higher than 300 eV, however, the binding energy at the

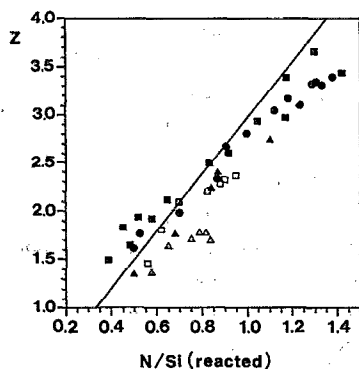


FIG. 8. The values of  $z$  [see Eq. (6)] obtained through the curve fitting of type  $B$  are plotted against the  $N/Si_{\text{reacted}}$  values. Solid squares indicate the data for 100 eV, solid circles indicate data for 200 eV, solid triangles indicate data for 300 eV, open squares indicate data for 500 eV, and open triangles indicate data for 1000 eV. The solid curve is a guide to the eye.

saturation does not reach these values. The binding energies obtained at 300, 500, and 1000 eV are 101.5, 101.2, and 100.7 eV, respectively. The FWHM of the spectrum for 100 and 200 eV initially increases, attains a maximum ( $\sim 4$  eV) at the dose of about  $2.5 \times 10^{15}$  ions/cm<sup>2</sup>, and decreases again. The final width is about 2.0 eV, which suggests that the spectrum consists mostly of the Si(4) component. For the higher energy beams, however, the width increases monotonically and saturates at a greater value. Their FWHMs at the saturation are 3.0, 2.8, and 2.3 eV for 300, 500, and 1000 eV, respectively. These values indicate that the spectra correspond to multichemical states.

These situations are well understood from the variation of the component ratios shown in Fig. 5. The width of the  $Si_{\text{reacted}}$  spectrum will reflect mixing of the different components. For 100 and 200 eV, broadening of the spectra becomes the largest at the ion dose of  $\sim 2.5 \times 10^{15}$  ions/cm<sup>2</sup>, where the four components of the reacted Si mix almost equally as seen in Fig. 5. The width of 2.0 eV at  $\sim 102.2$  eV for the final products is well correspondent to 1.9 eV of the main component Si(4). This indicates that the low energy beams produce the near stoichiometric compound  $Si_3N_4$ . This is consistent with the result of Park *et al.*<sup>10</sup> At 300 eV, the component ratios in the final product are 0.18, 0.21, 0.28, and 0.33 for Si(1), Si(2), Si(3), and Si(4), respectively. Such a mixing of the components gives a broad  $Si_{\text{reacted}}$  spectrum of 3.0 eV FWHM. At 500 eV, they are 0.26, 0.28, 0.27, and 0.18, respectively. The Si(4) component is the smallest in this case. At 1000 eV, the Si(1) component is the main one, the component ratios being 0.51, 0.28, 0.16, and 0.05, respectively. Then the width of the  $Si_{\text{reacted}}$  spectrum is narrower than that of 300 eV, but broader than for 100 eV.

The peak position of the  $Si_{\text{reacted}}$  spectrum may reflect the average nitrogen number bonded to one reacted Si atom. Here we can obtain the number  $z$  by

$$z = \frac{\sum_{n=1}^4 nI[Si(n)]}{\sum_{n=1}^4 I[Si(n)]}, \quad (6)$$

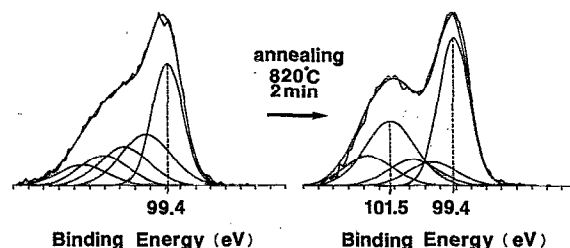


FIG. 9. The annealing effect. The  $Si2p$  XPS spectrum from a Si sample irradiated with the  $N_2^+$  beam of 1000 eV at room temperature changed into that spectrum in the right-hand side by heating at 820 °C for 2 min in UHV. The inner curves show intensities and positions of the five components  $Si(n)$  ( $n=0, 1, 2, 3$ , and 4).

but we do not show here the peak positions because they could not be determined definitely in some cases. Instead, the values of  $z$  obtained through the curve fitting of type  $B$  are plotted vs the  $N/Si_{\text{reacted}}$  values in Fig. 8. There is a linear relationship between both values, but the relation line shifts towards the lower side upon increasing the beam energy. The straight line in Fig. 8 represents an ideal relationship in that all nitrogen atoms bond to three Si atoms. At 100 and 200 eV, the relation lines are near to this ideal line, but the slope is a little lower. Under deviation from the line indicates that the nitrogen atoms bond less than three Si atoms. That is, the nitride layers include wrong (i.e., N–N) and/or unsaturated bonds ( $=Si-N$ , or  $-Si-N-Si-$ ) or defects. The data above the line which are observed for the low nitrogen content layers formed by the 100 and 200 eV beams may result from some unsuitable procedures used in the analysis. One of them is the assumption used in the fitting of type  $B$ , in which the widths of the Si(1), Si(2), and Si(3) components are the same to that of Si(4), but their widths of the Si(1), Si(2), and Si(3) components may be actually less than that of Si(4), though we have no method to determine them. In fact, the curve fitting of type  $A$  removes the upper deviation of the data. Another origin may be the relative sensitivity used for the  $Si2p$  and  $N1s$  spectra. The relative sensitivity for nitrogen to Si, which was obtained from the spectra of the  $Si_3N_4$  powder, appeared a little lower than what was used in the present analysis. This also works to remove the upper deviation. By those corrections, the data scattered in the left-low side will shift towards the right-hand side. The lines for 500 and 1000 eV are a little distant from the ideal line and the  $z$  values at the saturation are 2.4 and 1.7, respectively, which suggests that the nitride layers include much more defects than those formed by the lower energy beams. This is consistent with the results from Fig. 7.

Another interesting result is obtained in the plot of the  $N1s$  binding energies [ $E_B(N)$ ] vs the number  $z$ . Though the plot is not shown here, all data for the different beam energies, which are shown in Fig. 7, gather around a straight line given by

$$\begin{aligned} E_B(N) &= 0.38z + 396.72, & 1.0 \leq z \leq 3.0, \\ E_B(N) &= 397.86, & 3.0 < z < 4.0. \end{aligned} \quad (7)$$



This fact implies that the N1s binding energy reflects the bonding states with Si rather than the nitrogen content in the nitride layer.

Finally we have examined an annealing effect for the Si2p spectrum of the nitride film prepared with the 1000 eV beam. In Fig. 9, the spectra obtained before annealing and after 2 min heating at 820 °C are shown on the left- and right-hand sides, respectively. The shape of the spectrum changes dramatically by annealing. The spectrum before annealing is one broad peak having a big shoulder on the higher energy side, while after annealing, a peak separated from the 99.4 eV peak of the elementary Si appears at 101.5 eV. The five components given by curve fitting of type B are also shown in Fig. 9. The component ratios for Si(1), Si(2), Si(3), and Si(4) change from 0.24:0.18:0.14:0.09 to 0.10:0.11:0.27:0.12. The most intensive component among them is Si(1) before annealing, while Si(3) is the main one after annealing. This suggests that the nitrogen atoms trapped in unstable places such as unsaturated bondings, defects, and interstitial points move to make stable bonds at the regular lattice points by heating.

So far we have done the curve fitting of the spectra by using the five components of Si(0), Si(1), Si(2), Si(3), and Si(4), but it should be noticed that the nitride films produced at room temperature by irradiating the ion beams include many unstable states which cannot be represented by such ideal components. Thus the present analysis is qualitatively useful to see the change of the chemical states of the product during the reaction.

## V. SUMMARY

The nitridation process of a Si(100) surface at room temperature by low energy (100–1000 eV) nitrogen ion beams has been investigated. The N1s and Si2p XPS spectra of the surface were measured *in situ* during the progress of the reaction. The results are described as follows.

- (1) At all ion beam energies studied (100, 200, 300, 500, and 1000 eV), the intensity of the N1s peak increased linearly with the  $N_2^+$  dose in the initial stage, started to saturate at  $\sim 4 \times 10^{15}$  ions/cm<sup>2</sup>, and finally reached a constant value. The intensity curves as a function of the dose could be fitted by an analytical form of  $\alpha[1 - \exp(-bFt)]$ , which was derived from a rate equation of the reaction by assuming a simple model.
- (2) At ion energies lower than 300 eV, the N1s binding energy shifted from 397.1 to 397.9 eV upon increasing the nitrogen content, and the FWHM of the spectrum increased from 1.0 to 1.8 eV. At 1000 eV, however, the binding energy increased only up to  $\sim 397.4$  eV. The binding energy and the FWHM of the spectrum as a function of the ratio  $N/Si_{\text{reacted}}$  may give a measure of the imperfection of the silicon nitride film.
- (3) The surface nitrided with 100 and 200 eV ion beams showed a characteristic Si2p peak of the stoichiometric Si<sub>3</sub>N<sub>4</sub> compound at 102.1–102.4 eV, which means that the nitride layer was well separated from the unreacted Si substrate. The thickness of the nitride layer produced

with the 200 eV ion beam was about 1.5 nm. At higher energies, however, the Si2p XPS spectra did not show the distinct peak at 102.2 eV, while they tailed from the elemental Si peak into the chemically shifted region. These results suggest that the nitride films produced with high energy beams were nonstoichiometric compounds of a mixture of the Si(*n*) components with many defects. The plots of the  $z = \Sigma nI[Si(n)]/\Sigma I[Si(n)]$  values against  $N/Si_{\text{reacted}}$  showed a deviation from the ideal line. The films produced with the higher energy beams contain nitrogen atoms with unsaturated bondings with Si atoms.

- (4) These results show that a nitrogen ion beam of 100–200 eV produces a well-characterized thin Si<sub>3</sub>N<sub>4</sub> film on a Si substrate at room temperature, but at higher energy, the beam produces a thin film containing nonstoichiometric compounds SiN<sub>y</sub> ( $y < 1.3$ ) and many defects.

## ACKNOWLEDGMENTS

We would like to thank Professor Ch. Ottinger for the careful revision of the manuscript. This work was financially supported in part by grants in aid for scientific research from the Ministry of Education, Science, and Culture of Japan.

- <sup>1</sup>E. K. Hill, L. Kubler, J. L. Bischoff, and D. Bolmond, *Phys. Rev. B* **35**, 5913 (1987).
- <sup>2</sup>X. L. Zhou, C. R. Flores, and J. M. White, *Surf. Sci. Lett.* **274**, L268 (1992).
- <sup>3</sup>C. U. S. Larsson, C. B. M. Andersson, N. P. Prince, and A. S. Flodström, *Surf. Sci.* **271**, 349 (1992).
- <sup>4</sup>P. J. Chen, M. L. Colaizzi, and J. T. Yates, Jr., *Surf. Sci. Lett.* **274**, L605 (1992).
- <sup>5</sup>Ph. Avoris, F. Bozso, and R. J. Hamers, *J. Vac. Sci. Technol. B* **5**, 1387 (1987).
- <sup>6</sup>F. Bozso and Ph. Avouris, *Phys. Rev. B* **38**, 3937 (1988).
- <sup>7</sup>C. H. F. Peden, J. W. Rogers, Jr., N. D. Shinn, K. B. Kidd, and K. L. Tsang, *Phys. Rev. B* **47**, 15 622 (1993).
- <sup>8</sup>J. A. Taylor, G. M. Lancaster, A. Ignatiev, and J. W. Rabalais, *J. Chem. Phys.* **68**, 1776 (1978).
- <sup>9</sup>Y. S. Jo, J. Schultz, S. Tachi, S. Contarini, and J. W. Rabalais, *J. Appl. Phys.* **60**, 2564 (1986).
- <sup>10</sup>K. H. Park, B. C. Kim, and H. Kang, *J. Chem. Phys.* **97**, 2742 (1992).
- <sup>11</sup>D. H. Baek, H. Kang, and J. W. Chung, *Phys. Rev. B* **49**, 2651 (1994).
- <sup>12</sup>B. C. Kim, H. Kang, C. Y. Kim, and J. W. Chung, *Surf. Sci.* **301**, 295 (1994).
- <sup>13</sup>R. Kärcher, L. Ley, and R. L. Johnson, *Phys. Rev. B* **30**, 1896 (1984).
- <sup>14</sup>G. M. Ingo, N. Zaccchetti, D. della Sala, and C. Coluzza, *J. Vac. Sci. Technol. A* **7**, 3048 (1989).
- <sup>15</sup>D. Bolmont, J. L. Bischoff, F. Lute, and L. Kubler, *Appl. Phys. Lett.* **59**, 2742 (1991).
- <sup>16</sup>S. Hasegawa and P. C. Zahm, *J. Appl. Phys.* **58**, 2539 (1985).
- <sup>17</sup>M. P. Seah and W. A. Dench, *Surf. Interface Anal.* **1**, 2 (1979).
- <sup>18</sup>M. F. Hochella, Jr. and A. H. Carim, *Surf. Sci.* **197**, L260 (1988).
- <sup>19</sup>M. P. Seah, in *Practical Surface Analysis by Auger and X-ray Photoelectron Spectroscopy*, edited by D. Briggs and M. P. Seah (Wiley, New York, 1983), Chap. 5.
- <sup>20</sup>I. Kusunoki, M. Hiroi, T. Sato, Y. Igari, and S. Tomoda, *Appl. Surf. Sci.* **45**, 171 (1990).
- <sup>21</sup>I. Kusunoki and Y. Igari, *Appl. Surf. Sci.* **59**, 95 (1992).
- <sup>22</sup>I. Kusunoki, *Jpn. J. Appl. Phys.* **32**, 2074 (1993).
- <sup>23</sup>T. Aiyama, T. Fukunaga, K. Niihara, T. Hirai, and K. Suzuki, *J. Non-Cryst. Solids* **33**, 131 (1979).
- <sup>24</sup>R. D. Carson and S. E. Schnatterly, *Phys. Rev. B* **33**, 2432 (1986).
- <sup>25</sup>S. Hasegawa, L. He, T. Inokuma, and Y. Kurata, *Phys. Rev. B* **46**, 12 478 (1992).
- <sup>26</sup>G. A. Somorjai, *Chemistry in Two Dimensions: Surface* (Cornell University, London, 1981), p. 68.